35th European Modeling & Simulation Symposium
20th International Multidisciplinary Modeling & Simulation Multiconference

2724-0029 © 2023 The Authors.
doi: 10.46354/i3m.2023.emss.029

Comparison of a heat-air-moisture model with experiments for the drying behaviour of gypsum boards at higher temperatures

L. Weber[1,2,*], J. Herfurtner[1], H.-A. Jantzen[1] and U. Janoske[2]

[1]FH Münster, Stegerwaldstr. 39, Steinfurt, 48565, Germany
[2]Bergische Universität Wuppertal, Gaußstraße 20, Wuppertal, 42119, Germany

[*]Corresponding author. Email address: l.weber@fh-muenster.de

Abstract

Gypsum boards are commonly used materials and consume great amounts of energy in the production process. R&D is therefore needed to get a better understanding of the drying process and thus enabling for detailed optimization of drying parameters. Heat-air-moisture (HAM) models have been used in the last twenty years to simulate the hydrodynamic behaviour of construction materials. The model reported in literature has some limitations, the most important one being that the temperature in the porous media should remain below 80 °C. This work presents experimental data in comparison with results of the HAM model at higher temperatures up to 100 °C. A detailed comparison of the HAM model against experimental data for gypsum boards has yet been missing for those temperatures. The results show that the simulation model can correctly predict the course of the drying process when comparing water content over time. However, phenomenological differences arise in the temperature development over time.

Keywords: heat-air-moisture; experimental data; simulation; CFD; comparison

1. Introduction

Thermal drying is a central manufacturing step in the production of various industrial products. It is of great importance in the food industry, the building materials industry and the chemical industry. In the building materials industry, drying processes usually take place well above 100 °C.

The drying process is very energy intensive. In the 1990s, industrial drying processes contributed approximately 20 to 25 % to the total energy consumption of European countries such as Denmark or Germany (Defraeye, 2014; International Energy Agency [IEA]).

The production of gypsum products is an example of an energy intensive manufacturing process where a large part of the energy consumption falls to thermal drying. In the drying processes, it is necessary to optimize the energy consumption, production speed and product quality at the same time. For various gypsum products, the drying lines are set up in a tunnel construction, arranged in several floors. The drying line is well insulated from the outside. Thus, access from the outside is difficult or impossible. Experiments are therefore only possible with considerable effort. The high temperature and moisture load inside the dryer make locally resolved measurements with conventional measuring tools impossible. Here, the information is mostly limited to integral mass and energy balances.

Numerical modelling shows clear advantages when studying harsh environments. These models enable the calculation of locally resolved temperature and humidity distribution. Various boundary conditions can be applied to the model and thus parameter studies can efficiently be done.

Most challenging is the correct description of the physical effects that take place in the porous media (Kudra, 2004). These phenomena are strongly dependent on the material parameters that are mostly based on measurements. Therefore, each simulation model requires thorough validation (Defraeye et al., 2013). The aim of this work is to present experimental data of the drying process of a gypsum board. Additionally, a heat-air-moisture (HAM) Model is set up with own measurements to assess the possibility to use this model at temperatures from 40 °C to 100 °C. The comparison of this model against drying experiments at higher temperatures than atmospheric conditions has yet been missing in literature. We have chosen the temperature range up to 100 °C because calcium sulphate dihydrate (gypsum) is changing its level of hydration at higher temperatures due to endothermic reactions. This adds another phenomenon to the drying/dehydration of gypsum we first want to leave out.

The paper is structured as follows: Section 2 gives an overview over the state of the art of modelling drying processes. It follows section 3 with the presentation of the numerical modelling approach, the boundary conditions and the experimental setup used. Section 4 compares the results of the simulation model with the experimental data. Section 5 gives a critical opinion about the results and section 6 concludes the findings of this paper, the limitations of the presented model and gives an outlook on future work.

2. State of the Art

Vu and Tsotsas published a review of the mass and heat transport models for the analysis of the drying process in porous media (Vu & Tsotsas, 2018). They found that the most complete description of the physical processes is made by the theory of Whitaker (Whitaker, 1977). They stated that one major downside of the theory is the difficulty of obtaining the right transport parameters of the material under consideration.

In the following years, many derivatives of this theory were made and adopted to the needs of the specific case. One of them is the simulation of humidity transport in building materials. The European research project HAMSTAD from 2000 to 2003 standardized the simulation of building and room envelopes. The moisture absorption and release under atmospheric boundary conditions were simulated. (Hagentoft, 2002) and (Hagentoft et al., 2004) presented a heat-air-moisture (HAM) model that considers the transport of liquid water, water vapor and air through porous media. Fields for temperature and capillary pressure are solved. The material-specific relationship between absorbed moisture and the capillary pressure is used here to calculate a moisture distribution from the capillary pressure. Knowledge of this material behaviour is thus mandatory for the solution of the models and described in EN 15026 (Beuth, 2007).

This model has some limitations, which are described in detail in (Hagentoft, 2002). The most important one is that the temperature in the porous medium remains below 80 °C, mainly due to the reason that no liquid transport based on temperature gradients is modelled (Defraeye, 2011).

(Defraeye et al., 2011, 2012, 2013) used this model in various publications in the drying of gypsum boards with and without cardboard. However, the temperature ranges investigated did not exceed 20 °C and are far from the industrial boundary conditions of 130 °C to 320 °C.

One major challenge is to obtain the transport and storage parameters of the porous media. These are required inputs of the HAM-model and are normally results from pressure plate experiments and moisture diffusivity experiments (Janssen, 2022). These experiments take up to 75 days to be carried out. Recent research is being conducted on quicker and accurate methods to get these parameters (Deckers & Janssen, 2023).

Validations of the model against experiments with gypsum boards have only been carried out at atmospheric conditions (James et al., 2010). Validation of the model against temperatures above room temperature has not been carried out yet.

This paper presents an experimental setup and assesses its repeatability. We then present the results of the experiments between 40 °C and 100 °C and compare that to the numerical model to fill the gap in literature. After a complete validation of the model in the temperature range up to 100 °C, there can be done additional modelling to cope with the dehydration reactions.

3. Material and methods

Following the state-of-the-art analysis, the material and methods used in this study are presented here. The HAM modeling approach is employed to simulate the drying process. Experimental measurements were conducted to determine material properties and experimental boundary conditions such as thermal conductivity, heat capacity and heat transfer coefficients (HTCs). These were utilized in the subsequent simulations. Experimental data from a laboratory dryer, which allows for controlled temperature, humidity and fluid mechanical conditions, are used for validation. The drying process involves gypsum board samples with known dimensions and moisture content. The dryer operates in a flat plate setup, and various temperature and

humidity combinations are tested.

3.1. HAM-Modelling

The model considers liquid and vapor transport based on capillary pressure differences p_c and vapor transport based on thermal gradients.

The HAM-Model uses the capillary pressure as it is the true physical potential for capillary active media. Also, in association with the fact that flow transpires contrary to gradients of its driving potential, the capillary pressure is negative and defined as the difference between pressure in the liquid p_l and in the gaseous phase p_g:

$$p_c = p_l - p_g \tag{1}$$

The conservation equation of mass is:

$$\frac{\partial w}{\partial p_c}\frac{\partial p_c}{\partial t} + \nabla \cdot (\mathbf{g}_{\mathrm{m,l}} + \boldsymbol{g}_{m,v}) = 0 \tag{2}$$

The conservation of energy is:

$$c\rho_0 \frac{\partial T}{\partial t} + \left(c_l T \frac{\partial w}{\partial p_c}\right) \cdot \frac{\partial p_c}{\partial t} + \nabla \cdot (\boldsymbol{g}_{h,c} + \boldsymbol{g}_{h,a}) = 0 \tag{3}$$

In which $\boldsymbol{g}_{m,l}$ is the transport of liquid water based on the gradient of capillary pressure, $\boldsymbol{g}_{m,v}$ describes the transport of water vapor due to gradients of capillary pressure and temperature. $\boldsymbol{g}_{h,c}$ represents the heat conduction and $\boldsymbol{g}_{h,a}$ is the heat advection.

$$\boldsymbol{g}_{m,l} = -K_l \nabla p_c \tag{4}$$

$$\boldsymbol{g}_{m.v} = -K_{v,pc}\nabla \mathrm{p_c} - K_{v,T}\nabla T \tag{5}$$

$$\boldsymbol{g}_{h,c} = -\lambda \nabla T \tag{6}$$

$$\boldsymbol{g}_{h,a} = (c \cdot T)\boldsymbol{g}_{m,l} + (c_v T + L_v)\boldsymbol{g}_{m,v} \tag{7}$$

$$c = c_0 + \frac{1}{\rho_0} c_l w \tag{8}$$

With w the moisture content per volume, T the temperature, c_0 the heat capacity of the dry gypsum board, c_l the heat capacity of the liquid, L_v the enthalpy of vaporization of water, ρ_l the density of water and ρ_0 the density of the dry gypsum board.

$$K_{v,pc} = \frac{\delta_v p_v}{\rho_l R T} \tag{9}$$

$$K_{v,T} = \frac{\delta_v p_v}{\rho_l R T^2}\left(\rho_l L_v + p_c(T\gamma - 1)\right) \tag{10}$$

Here, δ_v is the permeability for vapor and γ is the normalised thermal derivative of the surface tension. For details of the derivation of the conservation equations and simplifications used see (Defraeye, 2011; Hagentoft et al., 2004; Janssen et al., 2007).

3.1.1. *Material properties*

The permeability K_l, describing the flow of liquid water is dependent on the capillary pressure. Figure 1 shows its course over p_c. Its values are obtained using a pore network simulation (Carmeliet et al., 1999; Carmeliet & Roels, 2001).

The liquid and vapor flow of each phase is strongly influenced by the corresponding permeability values that change with capillary pressure.

The moisture retention curve (Figure 1) gives the relation between capillary pressure and water content. It is also an important material property. For our modelling, the simulations use the values reported in (Defraeye et al., 2012).

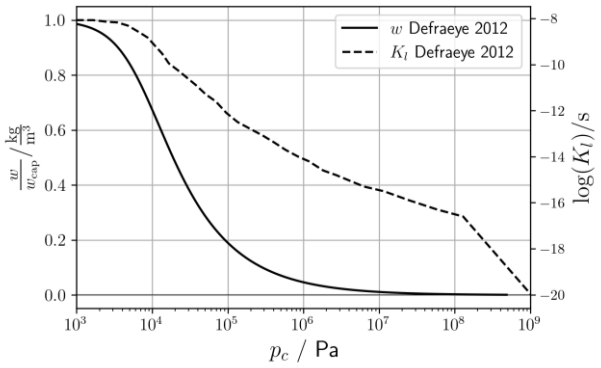

Figure 1. Water retention w and permeability for liquid water in the gypsum core over the capillary pressure (Defraeye et al., 2012)

The thermal conductivity λ was measured using a HotDisk® M1 device (Table 1). Measurements include different samples with different moisture content, so that a moisture dependent thermal conductivity was obtained:

$$\lambda = \lambda_0 + \lambda_w * w \tag{11}$$

The same device was used to measure the heat capacity c_0 of the dry sample. Additional properties of water are listed below (Table 2).

Table 1. Obtained material parameters for the wet gypsum core. Samples taken from the same production batch as the gypsum boards used for drying experiments.

Parameter	Value	Unit
w_{cap}	271	kg/m³
c_0	795.0	J/(kg*K)
λ_0	0.253	W/(m²*K)
λ_w	0.00101	W*m/(kg*K)
ρ_0	692	kg/m³

Table 2. Properties of water used for numerical modelling.

Parameter	Value	Unit
L_v	2.46e⁶	J/kg
c_v	1870	J/(kg*K)
ρ_v	0.588	kg/m³

3.1.2. Simulation domain

The domain under consideration is a one-dimensional representation of the gypsum board, aligned perpendicular to the plate surface. The domain is one half of a gypsum board. It consists of a gypsum core and a cardboard layer at the outer end. The gypsum core is resolved in 25 cells with a grading for smaller cells towards the cardboard, which is resolved as a specially adapted boundary condition.

3.1.3. Boundary conditions

The mass boundary condition only considers the transfer of water vapor:

$$g_{m,b} = \left(\beta * \left(p_{v,e} - p_{v,surf}\right)\right) * n \tag{12}$$

With $p_{v,e}$ being the external vapor pressure and $p_{v,surf}$ the partial pressure of water vapor at the surface, calculated using Kelvin's law:

$$p_{v,surf} = p_{v,sat}(T_{surf}) * \exp\left(\frac{p_{c,surf}}{\rho_l * R_v * T_{surf}}\right) \tag{13}$$

β is the mass transfer coefficient and n is the surface normal vector.

Heat transfer at the boundary is calculated as:

$$g_{h,e} = (H_e + LE_e) * n \tag{14}$$

$$H_e = \alpha * (T_e - T_{surf}) \tag{15}$$

$$LE_e = \left(c_v T_{surf} + L_v\right) * E_e \tag{16}$$

The effect of the cardboard is modelled by assuming a negligible mass and heat storage in the cardboard. We equate the mass flow over the cardboard with the mass flow leaving the cardboard (figure 2). This is also done for the heat flow. The new surface values can then be calculated with:

$$p_{v,surf} = \frac{\beta\, p_{v,e} + k\, p_{v,i}}{\beta + k} \tag{17}$$

$$\mathrm{T_{surf}} = \frac{\alpha \mathrm{T_e} + \frac{\lambda}{s}\,\mathrm{T_i}}{\alpha + \frac{\lambda}{s}} \tag{18}$$

Here, k is the diffusion through the cardboard, $p_{v,i}$ is the vapor pressure at the surface of the gypsum board, s the thickness of the cardboard, λ the heat transfer coefficient of the cardboard and T_i the temperature at the gypsum surface.

$$k = \frac{\delta_v \mu}{s} \tag{19}$$

With δ_v being the diffusion coefficient of water vapor in air and μ being a material dependent factor describing the relation of diffusion through a material to the diffusion through air.

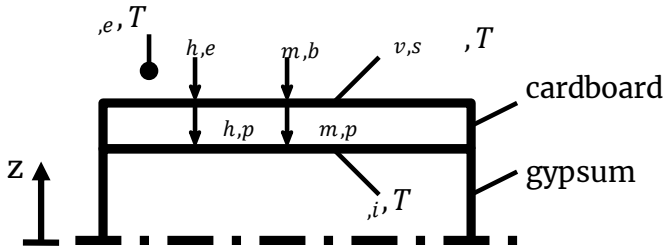

Figure 2. Modelling of the additional resistance of the cardboard

3.1.4. Solving method

The finite volume method (FVM) is chosen for the special discretization. This has advantages over the finite element method as it leads to more monotonic moisture fronts and therefore better convergence. On the other hand, the FVM does not directly calculates the values at the boundary and additional approximation is needed (Janssen et al., 2007). This is compensated with a high mesh resolution towards the boundary. For temporal discretization the first order backwards Euler method is used.

The equations 2 – 11 show a strong dependence of material parameters on the capillary pressure or the temperature or both at the same time. Examples are the water content w, the permeability for liquid water K_l, the permeability for water vapor with respect to gradients in capillary pressure $K_{v,pc}$, its equivalent with respect to thermal gradients $K_{v,T}$ and the thermal conductivity λ.

To solve these nonlinear equations the Picard iterative scheme is used in our model. It updates the values for p_c and T, using the old material parameters. Then it calculates the material parameters w, K_l, $K_{v,pc}$, $K_{v,T}$ and λ according to p_c and T. It then checks for convergence criteria and then repeats in case of a failure or moves on to the next time step. If the loop exceeds a specified maximum of iterations, the time step is reduced, and the loop restarted. The alternative scheme would be a Newton-Raphson procedure. This requires the numeric calculation of the derivatives of the material parameters and is therefore more difficult to implement and computationally expensive. In the case of HAM-modelling, none of the schemes clearly performs better than the other one (Mehl, 2006). The Picard iterative scheme is choses as it is straight forward and faster.

3.2. Testing facility

Results from the simulations are validated against experimental data from the laboratory dryer. The dryer can maintain a constant atmosphere inside, so that different boundary conditions of the simulation can be tested. The dryer works in a closed-circuit principle and regulates temperature and humidity of the drying atmosphere. The dryer can work in the flat plate setup

or with an array of impinging jets.

The drying media are placed on three pins to block as little surface area of the probe as possible. The sample holder is connected via a linkage to a precision force transducer, which continuously records the weight of the sample. Two temperature sensors are inserted in the sample, one in the centre and one at the surface.

3.3. Setup for the comparison

The temperature range for the investigation is 40 °C to 100 °C in steps of 20 °C. Humidities are varied between 10 % RH and 30 % RH in steps of 10 % RH. In addition to these 12 experiments, four repetitions were carried out to assess the repeatability.

The sample is a gypsum board with the dimensions of 360 mm * 360 mm*12.5 mm. 40 % of the dry weight was added as deionized water. After 2 days the wetted gypsum board was used for the drying experiment. The dryer was in the flat plate setting with 6.7 m/s wind speed parallel to the surface of the probe. The air flow at the gypsum plate was separated from the main air flow in the climate chamber by a channel construction. To reduce air flow turbulence, the setup was operated in suction mode.

The distribution of the heat transfer coefficient along the surface of the plate was measured with a dry gypsum plate. Over the length of the sample, 12 thermocouples were inserted in the plate. Using the known heat capacity of the dry gypsum board, one can calculate the heat transfer coefficient at the location of the corresponding thermocouple. The HTC in our case was 54 W/m²K. The mass transfer coefficient was determined applying the Reynolds analogy for heat and mass transfer.

4. Results

The experiments were divided into two groups:

- Repeating one experiment many times to get a sense for the repeatability.
- Varying temperature and humidity according to section 3.3.

4.1. Repeatability

When comparing differences between experiments where the boundary conditions are varied, it is a requirement to observe the repeatability of the experimental method. In the following section, the weight over time and the temperature over time of the different samples is shown (compare figure 3).

The plots of the weight over time start at slightly different values in the beginning. That is since the samples took up different amounts of water in the preparation. The range at the start is from 12.28 kg/m² to 12.37 kg/m² or 0.7 % difference, respectively.

The weight settles at slightly different levels ranging from 8.92 kg/m² to 9.05 kg/m². The samples differ 1.4 % in their respective dry weight.

The derivative of the weight over time is the drying rate. They are in close agreement with each other (Figure 4). At high residual moistures, correspondingly the start of the experiment, the plot is very sensitive to the tangent at t=0 sec. (Figure 3), so unphysical outliers of the mass at the start of the measurement have a big impact of the start of the curves shown in figure 4.

The temperatures show larger deviations during the experiment. After the sample heated up, the temperature at t = 800 sec. spreads from 55.3 °C to 57.7 °C. This difference is almost constant up to t = 5600 sec. where temperature ranges from 69.5 °C to 71.3 °C. The results show that samples that have been warmer take up less heat (same principle as in Equation 14) and take longer for drying.

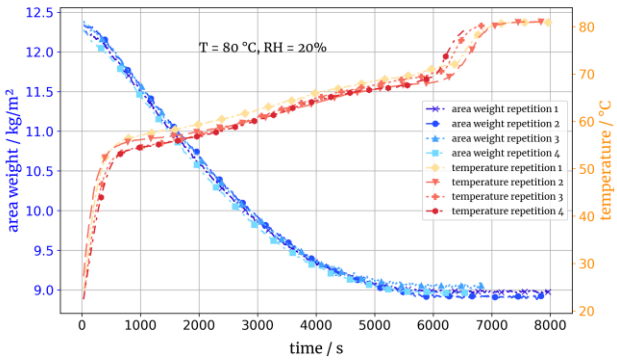

Figure 3. Repetition of the experiment under the same conditions to access repeatability

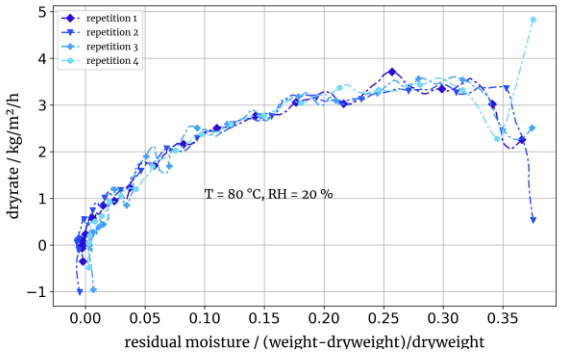

Figure 4. Drying rates for the repeated experiments over the residual moisture.

4.2. Parameter study

Figure 5 shows the results of the drying experiments with varying temperatures and humidities. Each column represents a constant temperature, each row a constant humidity. The temperatures of the experiment and the simulation are shown in the red curves, the weight of the sample in both simulation and experiment is shown in

blue.

The comparison of the experiments and simulations under different boundary conditions shows good matching for 80 °C and 100 °C ambient temperature for all humidities. The results differ more at 60 °C and even more at 40 °C.

The temperatures in the simulation mostly surpass the experimental data for lower temperatures. It shifts in the other direction for higher temperatures and for 60 °C we obtain close agreement between the two data sets. At 100 °C, there is a difference of approximately 10 °C where the simulation predicts higher values.

In a comparison of the experimental temperature curves with those of the simulation, phenomenological differences become apparent. The simulation model predicts a constant temperature plateau and therefore a constant drying rate. This is known as the "constant drying period" in the theory. It occurs when the surface of the porous media is wet throughout this time. After that, the results from the simulation show a decrease in drying rate, known as the second drying phase, where the surface begins to dry out so that heat and moisture must overcome additional resistances to get to the liquid water. As a result, the drying slows down.

The experimental data for the temperature curves show a constant warming up sample. A constant drying phase (compare also Figure 3) was not observed in our experiments.

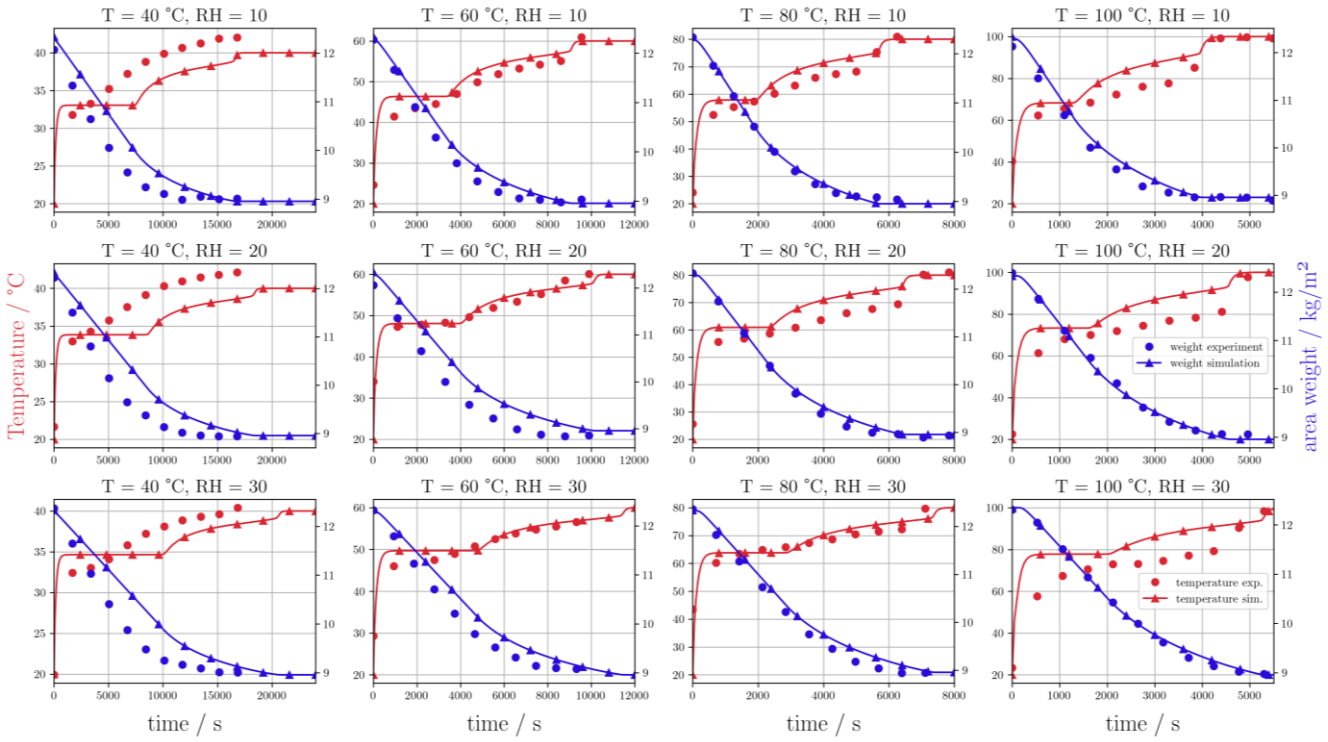

Figure 5. Comparison between results from the experiment and the simulation

5. Discussion

The results of the parameter study show trends in the degree of agreement as well in the weight loss as also in the temperature over time. The weight fits better for higher temperatures and shows a divergence towards lower temperatures. One exception is the experiment with 100 °C and 10 % RH, but here the starting mass of the sample was lower, so a constant offset arose.

Also, the simulation predicts temperatures that are too low at 40 °C and ones that are too high at 100 °C with some good agreement at 60 °C and 80 °C. The small but noticeable drift in both metrics indicates one or more slightly incorrectly selected material parameters. The moisture retention curve and the permeability for liquid water for example have a big impact on the result of the simulation. These are specific for each material but hard to obtain. The values used here are taken for gypsum boards reported in literature and may therefore differ slightly from the gypsum boards used in our experiments.

Regarding the phenomenologically differences in the temperature development between the experiment and the simulation, a variation in numeric input parameters has been conducted to give an insight, which parameters in the model have an impact on temperature development. It can be seen in figure 3 that

temperature development is different, despite having the same temperature, humidity and air velocity conditions. In the flat plate setup, the air flow reacts very drastically on small changes of the pitch angle of the plate. Reattachment zones from the blunt edge largely change within very tiny angle adjustments. Thus, the heat transfer coefficient changes. With an optimised sample holder or placing routine, this influence can be minimized.

Porous media with a high resistance to liquid flow does not show the wet bulb temperature at its surface during drying. The pseudo wet bulb temperature is a concept to describe surface temperatures of porous media with resistance to fluid transport in the drying process. A little change in resistance changes the surface temperature and therefore the core temperature as well.

Based on the assumptions that the heat transfer coefficient and the permeability of liquid water have a significant impact on the development of the temperature, these were varied first:

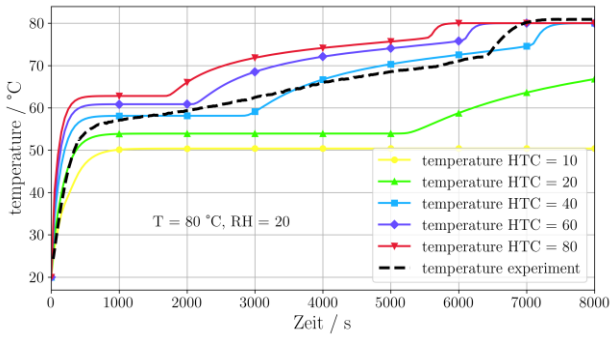

Figure 6. Impact of the variation of the heat transfer coefficient on the temperature development.

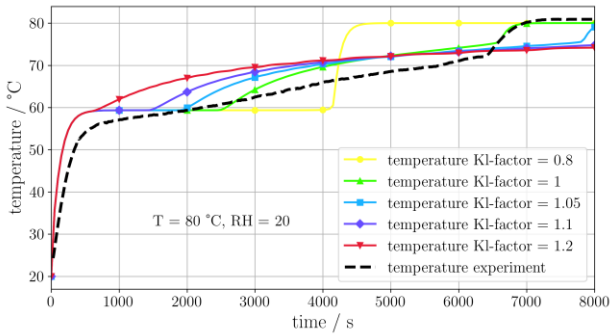

Figure 7. Impact of the variation of the liquid permeability K_l on the temperature development

Figure 6 shows the impact of variations in the heat transfer coefficient (HTC) and figure 7 the same for variations of permeability of liquid water K_l. The first was changed in steps of 10, 20,40, 60 and 80 W/m²K and the latter was multiplied by a factor of 0.8, 1, 1.05, 1.1 and 1.2 in logarithmic scale over the complete range of capillary pressure (comp. fig. 1). The results of the variation show that a rise of the HTCs results in a higher temperature during the plateau phase. The drying is faster for higher HTCs. A change of K_l result in shorter plateaus for the factors larger than 1 and for longer plateaus for factors below 1. For the highest factor, the plateau is completely gone. Though the length of the constant temperature phase can be varied, the temperature level stays constant.

The experimental results obtained from the laboratory dryer show reasonably good results regarding the repeatability in drying rate. The level of the temperatures inside the gypsum board seems to be very sensitive towards the heat transfer coefficient. As the drying rate is in very close agreement for all four experiments, the same amount of energy leaves the system in form of evaporation. That in consequence means that the same amount of energy is brought into the system. To meet the physical laws of heat transfer, the temperature of the porous media must rise in coexistence with a higher heat transfer coefficient.

The slight offset in the dry weight of the samples in the end of the drying might be an effect of dehydration of the gypsum board during manufacturing. This dehydration has been reversed when wetting the sample. All the experiments showed the effect that the gypsum board did not reach the same dry weight in the end of the experiment as it had before been wetted. This dehydration seems to occur to different degrees in the different plates.

6. Conclusions

This work presents a way to validate the results of a HAM simulation in the temperature range between 40 °C and 100 °C. The model used is a combination of own measurements (see table 1 & 2) and transport parameters according to Defraeye (Defraeye et al., 2012). The parameter study shows good agreement between experimental data and the numeric model in regards of water content over time. One limitation of this HAM modelling is the prediction of the temperature development in the gypsum board. Whereas the simulations show a temperature plateau, the experiments have a slow increase in temperature. In addition, an improved sample holder can lead to better and closer repeatability of the temperature development over time.

This work is still limited in temperature in the porous media to be below 100 °C. Above that threshold, there are endothermic dehydration reactions which require additional modelling.

For gypsum boards, there seems to be no reason to limit temperatures in the porous media to less than 80 °C. The effect of liquid flow based on thermal gradients is small, as gypsum boards do not develop a steep gradient in temperature.

Future work will focus on a systematic approach for obtaining permeability parameters from experiments. For reaching closer agreement between experiments and simulations, one must obtain his own values for the

permeabilities of liquid flow and vapor flow.

In addition, the performance of the simulation model should be evaluated for temperatures up to 250 °C and for water vapor mixing ratios up to 500 g/kg.

Acknowledgements

Most of the equipment used in this work was supported by the funds of the BMBF of Germany in the scope of the project "Gipsplattentrocknung" (13FH064PX8).

References

Beuth (2007). *Wärme- und feuchtetechnisches Verhalten von Bauteilen und Bauelementen - Bewertung der Feuchteübertragung durch numerische Simulation* (DIN EN 15026:2007-07). DIN EN 15026:2007-07. Beuth Verlag GmbH. https://www.beuth.de/de/norm/din-en-15026/94169966

Carmeliet, J., Descamps, F., & Houvenaghel, G. (1999). A Multiscale Network Model for Simulating Moisture Transfer Properties of Porous Media. *Transport in Porous Media*, *35*(1), 67–88. https://doi.org/10.1023/A:1006500716417

Carmeliet, J., & Roels, S. (2001). Determination of the Isothermal Moisture Transport Properties of Porous Building Materials. *Journal of Thermal Envelope and Building Science*, *24*(3), 183–210. https://doi.org/10.1106/Y6T2-9LLP-04Y5-AN6T

Deckers, D., & Janssen, H. (2023). Development and validation of the steady state centrifuge experiment for the moisture retention curve of porous building materials. *Journal of Building Physics*, *47*(1), 36–61. https://doi.org/10.1177/17442591231178778

Defraeye, T. (2011). *Convective heat and mass transfer at exterior building surfaces* [Dissertation]. Katholieke Universiteit Leuven, Leuven.

Defraeye, T. (2014). Advanced computational modelling for drying processes – A review. *Applied Energy*, *131*, 323–344. https://doi.org/10.1016/j.apenergy.2014.06.027

Defraeye, T., Blocken, B., & Carmeliet, J. (2011). Analysis of convective heat and mass transfer coefficients for convective drying of a porous flat plate by conjugate modelling. *International Journal of Heat and Mass Transfer.* Advance online publication. https://doi.org/10.1016/j.ijheatmasstransfer.2011.08.047

Defraeye, T., Blocken, B., & Carmeliet, J. (2013). Influence of uncertainty in heat–moisture transport properties on convective drying of porous materials by numerical modelling. *Chemical Engineering Research and Design*, *91*(1), 36–42. https://doi.org/10.1016/j.cherd.2012.06.011

Defraeye, T., Houvenaghel, G., Carmeliet, J., & Derome, D. (2012). Numerical analysis of convective drying of gypsum boards. *International Journal of Heat and Mass Transfer*, *55*(9-10), 2590–2600. https://doi.org/10.1016/j.ijheatmasstransfer.2012.01.001

Hagentoft, C.-E. (2002). *HAMSTAD- WP 2 Modeling.* Chalmers University of Technology.

Hagentoft, C.-E., Kalagasidis, A. S., Adl-Zarrabi, B., Roels, S., Carmeliet, J., Hens, H., Grunewald, J., Funk, M., Becker, R., Shamir, D., Adan, O., Brocken, H., Kumaran, K., & Djebbar, R. (2004). Assessment Method of Numerical Prediction Models for Combined Heat, Air and Moisture Transfer in Building Components: Benchmarks for One-dimensional Cases. *Journal of Thermal Envelope and Building Science*, *27*(4), 327–352. https://doi.org/10.1177/1097196304042436

International Energy Agency. 2019 Global Status Report for Buildings and Construction.

James, C., Simonson, C. J., Talukdar, P., & Roels, S. (2010). Numerical and experimental data set for benchmarking hygroscopic buffering models. *International Journal of Heat and Mass Transfer*, *53*(19-20), 3638–3654. https://doi.org/10.1016/j.ijheatmasstransfer.2010.03.039

Janssen, H. (2022). Comment on Cabrera et al. A User-Friendly Tool to Characterize the Moisture Transfer in Porous Building Materials: FLoW1D. Appl. Sci. 2020, 10, 5090. *Applied Sciences*, *12*(3), 1123. https://doi.org/10.3390/app12031123

Janssen, H., Blocken, B., & Carmeliet, J. (2007). Conservative modelling of the moisture and heat transfer in building components under atmospheric excitation. *International Journal of Heat and Mass Transfer*, *50*(5-6), 1128–1140. https://doi.org/10.1016/j.ijheatmasstransfer.2006.06.048

Kudra, T. (2004). Energy Aspects in Drying. *Drying Technology*, *22*(5), 917–932. https://doi.org/10.1081/DRT-120038572

Mehl, S. (2006). Use of Picard and Newton iteration for solving nonlinear ground water flow equations. *Ground Water*, *44*(4), 583–594. https://doi.org/10.1111/j.1745-6584.2006.00207.x

Vu, H. T., & Tsotsas, E. (2018). Mass and Heat Transport Models for Analysis of the Drying Process in Porous Media: A Review and Numerical Implementation. *International Journal of Chemical Engineering*, *2018*, 1–13. https://doi.org/10.1155/2018/9456418

Whitaker, S. (1977). Simultaneous Heat, Mass, and Momentum Transfer in Porous Media: A Theory of Drying. *Advances in Heat Transfer*(13), 119–203. https://doi.org/10.1016/S0065-2717(08)70223-5